

A 4th Year Project Report for Professor J. Rogers

Voltage-Controlled Oscillators in Cable Tuners

April 9, 2003

Kevin Cheung

Abstract

The desire for wide bandwidth receivers is realized in the integrated cable tuner, a receiver capable of tuning signals ranging from 50 MHz to 850MHz. This project implements a 1.85 GHz voltage-controlled oscillator, the component that provides the reference tone that enables the mixers to upconvert, downconvert, or image reject the signal as required. Implemented monolithically in 0.18 μm CMOS technology, MOS varactors were designed to achieve maximum tuning range. On-chip spiral inductors achieving a Q of 5.22 were also created. Lastly, a 3-stage polyphase filter was implemented to provide a 90° phase shift for the image reject mixers. The VCO can tunes between 1.84 GHz and 1.88 GHz and exhibits phase noise of -109.9 dBc/Hz at a 100 kHz offset and -136 dBc/Hz at a 1 MHz offset.

Table of Contents

List of Figures	i
List of Tables	ii
Acknowledgements	iii
1.0 Introduction	1
2.0 Overview of the Integrated Cable Tuner	2
2.1 General Objectives.....	2
2.2 Top Level Design.....	2
2.3 Why Use 0.18 μm CMOS?.....	3
3.0 The Voltage-Controlled Oscillator	5
3.1 The Two VCO's.....	5
3.2 Specifications.....	7
3.3 Oscillator Basics.....	7
3.4 Phase Noise.....	8
4.0 Oscillator Design Process	11
4.1 The Negative G_m Oscillator.....	11
4.2 LC Resonator.....	12
4.3 Varactors.....	14
4.4 Inductors.....	19
4.5 Polyphase Filters.....	22
4.6 Design Summary.....	25

5.0	Simulations and Results	26
5.1	Transient Response	27
5.2	Phase Noise	28
5.3	Results Summary.....	29
6.0	Future Work	30
7.0	References	31

List of Figures

Figure 1: Cable Tuner Block Diagram.....	3
Figure 2: Second VCO and Image Reject Mixers.....	6
Figure 3: Block Diagram of a Feedback Loop.....	8
Figure 4: Negative G_m Oscillator topology.....	12
Figure 5: The LC Resonator.....	14
Figure 6: Cross-Section of a Varactor.....	15
Figure 7: Varactor Test Bench.....	16
Figure 8: Smith Chart of Varactor's Input Impedance.....	17
Figure 9: Normalized Imaginary Impedance vs. Tuning voltage of Varactors.....	18
Figure 10: Inductor Geometry.....	21
Figure 11: 3-Stage Polyphase Filter.....	23
Figure 12: Polyphase Filter Testbench.....	23
Figure 13: Polyphase Filter Testbench Output.....	24
Figure 14: Complete VCO.....	25
Figure 15: VCO Operating Points.....	26
Figure 16: Transient Output Signal for $V_{\text{tune}} = 0V$	27
Figure 17: Phase Noise Response.....	28

List of Tables

Table 1: Voltage-Controlled Oscillator Specifications	7
Table 2: Inductor Geometry	20
Table 3: Inductor Properties at 1.85 GHz	21
Table 4: Summary of Results	29

Acknowledgements

I would like to extend my gratitude and appreciation to all those who have helped to guide this project in the right direction.

Most importantly, my supervisor,

Dr. John Rogers

His trusty side-kick,

Steve Knox

My talented and always motivated group members,

Derek Van Gaal

Christina George

Vince Karam

Mark Fairbarn

Bi Pham

And, of course,

Senegal

Denmark

Nepal

...those late nights spent together were special.

1.0 Introduction

Society has always imposed high demands on research and development in the communication industry. Faster and more reliable means of communication are constant requirements of businesses and ordinary people alike. With the advent of technology and the rapid growth of the Internet, the ability to instantaneously share vast quantities of information across the world has become an everyday reality. Today, the Internet and other novel technologies touch every aspect of our life: from work and school, to home and entertainment. As a result, increased bandwidth, lower power consumption, and further cost-effectiveness have become highly sought commodities.

To meet these demands, wide bandwidth solutions must be further developed. Integrated cable tuners are one such solution. Cable signals are no longer used to just carry television signals. Today, high speed Internet, digital television, and voice over IP (VOIP) can be transmitted over the same coaxial cables running into the home. The creation of a cost-effective cable tuner capable of receiving a wide spectrum of signals would enable these luxuries to be available in every home. Through this project, the voltage controlled oscillators for these cable tuners will be investigated and designed in 0.18 μm CMOS technology.

2.0 Overview of the Integrated Cable Tuner

Integrated cable tuners are receivers designed to receive a wide range of frequencies. While ordinary receivers may have an operational range of a couple of megahertz (10^6 Hz), cable tuners are designed to function over a range of about a gigahertz (10^9 Hz). This increased bandwidth means that more information can be transferred along the same cable. Practically, this will mean faster downloads and the integration of high speed Internet access, digital television, and voice over IP (VOIP) services into a single device. Functionality can be further integrated as the power supply for the device can be provided over the same cable. Designed for home use, integrated cable tuners would reside in a wall-mounted box just outside of the home.

2.1 General Objectives

The cable tuner must be able to receive a wide spectrum of signals ranging from 50 MHz to 850 MHz and effectively select and amplify the desired channel. This signal must be translated through various intermediate frequencies to baseband with a minimal introduction of noise. The final cable tuner must be able to work reliably in a variety of temperature ranges and exhibit linearity over the entire frequency range. In addition, low power consumption and cost-effectiveness are essential for market viability.

2.2 Top Level Design

The cable tuner has been subdivided into a number of smaller components to simplify the design. As illustrated by the block diagram in *Figure 1*, the cable signals enter the home through a standard coaxial cable. The received signals are first amplified by a low-noise amplifier (LNA) and then sent through the first mixer where they are

translated to a single IF frequency of 1.8 GHz. This signal is then sent off chip to a bandpass filter where image signals and noise are eliminated. The refined signal is amplified again and then sent through the image reject mixer to down convert the signal from the IF frequency of 1.85 GHz to a second IF frequency of 45 MHz.

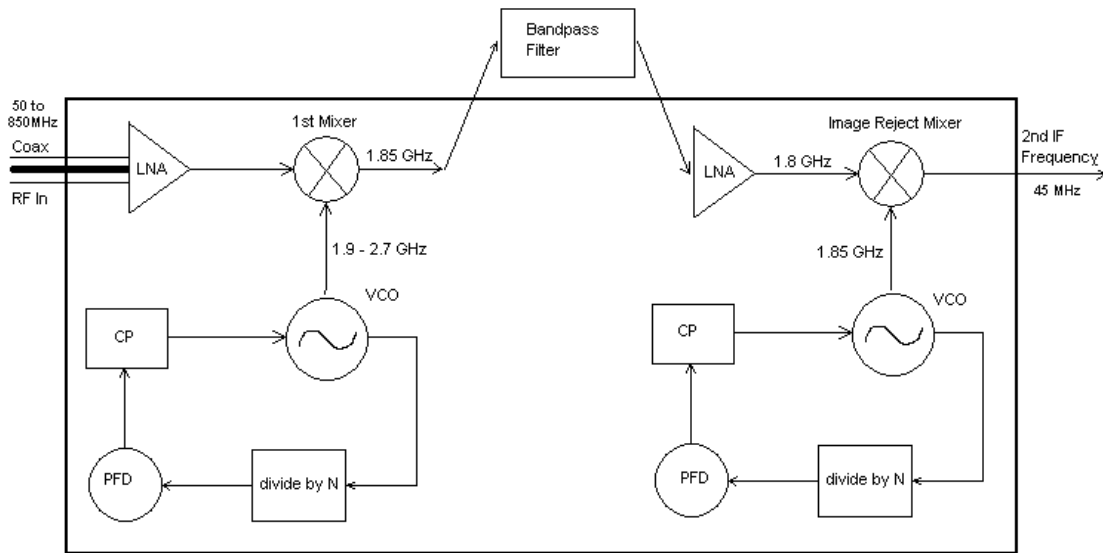


Figure 1: Cable Tuner Block Diagram

As the design of the complete cable tuner is a quite involved process, each group member was assigned a specific component of the cable tuner. I was responsible for the design of the voltage-controlled oscillators (VCOs).

2.3 Why Use 0.18 μm CMOS?

This project was completed using 0.18 μm CMOS technology since CMOS offers several advantages over bipolar technology and because the technology was readily available in the labs. CMOS, first of all, offers the potential for larger scale integration [9] and higher operating frequencies. This, combined with lower power consumption and lower voltage requirements, may result in increased economical value [9]. CMOS,

furthermore, enables the implementation of mixed analog-digital designs resulting in improved functionality and further integration.

3.0 The Voltage-Controlled Oscillator

The voltage-controlled oscillator generates a periodic signal that can be used for many analog and digital applications, wherever a reference tone is required. For the cable tuner, the voltage-controlled oscillators produce a stable sinusoid signal that act as a reference frequency for the mixers. These reference frequencies enable the mixers to translate the input signal to the desired intermediate frequency [1]. As illustrated in the block diagram above (*Figure 1*), there are two such oscillators in the cable tuner. Both oscillators have the same basic design differing primarily in their individual oscillating frequencies. In addition, each VCO is part of a phase-locked loop. The phase-locked loop provides the tuning voltage to control the frequency of oscillation. It also works through feedback to constantly correct itself in case of variations in temperature or noise.

3.1 The Two VCO's

There are two voltage-controlled oscillators in the cable tuner, and each supplies a reference frequency for the mixers in the circuit. The first mixer up converts the incoming RF signal, which can range between 50 MHz and 850 MHz, to the common IF frequency of 1.85 GHz. The first voltage-controlled oscillator, consequently, has a very wide tuning range; it must be able to tune between 1.9 GHz and 2.7 GHz.

The second voltage-controlled oscillator has two main purposes. First, it provides the reference frequency for the image reject mixer to down convert the signal from the first IF frequency of 1.85 GHz to the second IF frequency of 45 MHz. Second, as illustrated below in *Figure 2*, the IF signal is actually split and mixed to the second IF frequency by two frequencies that differ by a ninety-degree phase shift. The summation

of these resulting signals enables the cancellation of the image signals formed around the carrier as a result of the mixing. The second voltage-controlled oscillator has a tuning range of 1.82 GHz to 1.87 GHz and produces multiple sinusoids, each shifted in phase by ninety degrees. For the purposes of this project, more work was dedicated to the second voltage-controlled oscillator.

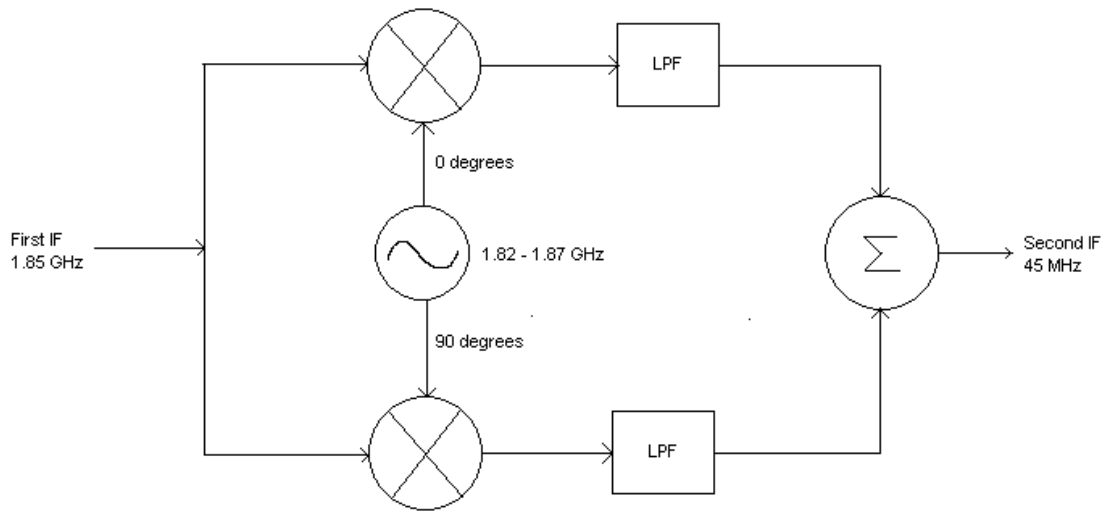


Figure 2: Second VCO and Image Reject Mixers

3.2 Specifications

In addition to the tuning requirements specified above, the voltage-controlled oscillator must meet the following specifications:

Table 1: Voltage-Controlled Oscillator Specifications

Characteristic	Specification
Power Supply	3.3 VDC
Current Drain	$I_{\text{Bias}} \leq 15 \text{ mA}$
Oscillator Gain	$K_{\text{VCO}} \leq 250 \text{ MHz/V}$
Phase Noise	at 100 kHz, $\text{PN} \leq -103 \text{ dBc/Hz}$ at 1 MHz, $\text{PN} \leq -123 \text{ dBc/Hz}$
Tuning Voltage	$0.3 \text{ V} \leq V_{\text{tune}} \leq 3.0 \text{ V}$

3.3 Oscillator Basics

A basic voltage controlled oscillator is comprised of two main components: a resonator and a feedback loop. The resonator starts the oscillations when supplied with an impulse current, usually provided by noise in the system. The oscillations, however, quickly fade as a result of damping, and, consequently, a feedback loop is required to sustain the oscillations.

The feedback loop is illustrated by the block diagram in *Figure 3* below.

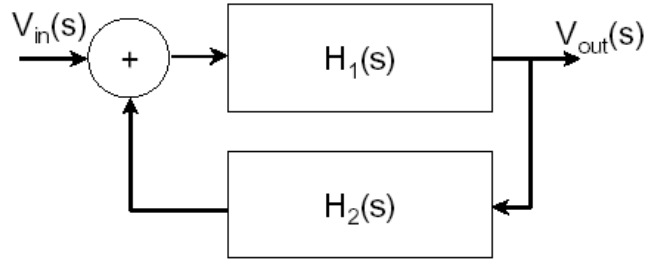


Figure 3: Block Diagram of a Feedback Loop

From this diagram, the gain of the system can be represented by the following equation [1]:

$$\frac{V_{out}(s)}{V_{in}(s)} = \frac{H_1(s)}{1 - H_1(s)H_2(s)} \quad (1)$$

When the denominator $1 - H_1(s)H_2(s)$ equals zero, the gain becomes infinity and the conditions for oscillation are met. To sustain oscillations with constant amplitude, the gain must be equal to 1 and the phase around the loop must be equivalent to 2π radians ($0^\circ, 360^\circ$, etc) [2]. Thus the conditions of oscillation can be summarized as follows [1]:

$$\begin{aligned} |H_1(s)H_2(s)| &= 1 \\ \angle H_1(s)H_2(s) &= 2n\pi \end{aligned} \quad (2)$$

The general approach is to generate a negative resistance in parallel to the resonator circuit. This overcomes the resistance of the circuit and sustains the oscillations.

3.4 Phase Noise

Illustrated by “skirts” around the carrier frequency, phase noise is the random fluctuations in the output frequency of the VCO [6]. In the cases of the two VCOs where output signal frequency is extremely important, excessive phase noise can result in incomplete image rejection or up-conversion or down-conversion to an undesired IF

frequency. The main contributor to phase noise is the LC resonator, hence the importance of a high quality factor Q. Improved inductors and large voltage swing of the oscillations help to minimize the relative phase noise.

The following is an estimate of the oscillator's phase noise using Leeson's equation [6]. The values used are the results obtained from simulation.

$$PhaseNoise = \left(\frac{|H_1| \omega_o}{2Q\Delta\omega} \right)^2 \left(\frac{|N_{in}(s)|^2}{2P_s} \right) \quad (3)$$

where $P_s =$ signal power of carrier

$|N_{in}(s)|^2 =$ input noise (kT)

$H_1 = 1$

First, we find the parallel resistance of the resonator, which ends up being equal to the parallel resistance of the inductor since the varactor's resistance is extremely high.

$$\begin{aligned} R_p &= \left(\frac{1}{r_{p,cap}} + \frac{1}{r_{p,ind}} \right)^{-1} \\ &= \left(\frac{1}{\infty} + \frac{1}{r_{p,ind}} \right)^{-1} \\ &= r_{p,ind} \\ &= Q_{ind} \omega L \\ &= (5.22)(2\pi)(1.85GHz)(3nH) \\ &= 182.03\Omega \end{aligned}$$

Next, the signal power of the carrier can be calculated as follows,

$$\begin{aligned} P_s &= \frac{V_{\tan k}^2}{2R_p} \\ &= \frac{(3.5V)^2}{(2)(182.03\Omega)} \\ &= 33.648mW \end{aligned}$$

And the quality factor of the oscillator Q_{osc} can be calculated,

$$\begin{aligned}
Q_{osc} &= R_p \sqrt{\frac{C}{L}} \\
&= (182.03\Omega) \sqrt{\frac{2.5pF}{3nH}} \\
&= 5.255
\end{aligned}$$

Since, $|N_{in}(s)|^2 = kTF$, where k is Boltzmann's constant (1.38×10^{-23} J/K), T is temperature in Kelvin (298 K), and F is the noise factor (approximated to 5dB), we can solve for phase noise using Leeson's equation,

$$\begin{aligned}
PhaseNoise &= \left(\frac{|H_1| \omega_o}{2Q\Delta\omega} \right)^2 \left(\frac{kT}{2P_s} \right) \\
&= \left(\frac{(1)(1.85GHz)}{(2)(5.255)(1MHz)} \right)^2 \left(\frac{(1.38 \times 10^{-23})(298K)(5dB)}{(2)(33.648mW)} \right) \\
&= 9.467 \times 10^{-15}
\end{aligned}$$

Converting this to decibels,

$$\begin{aligned}
PN_{dB} &= 10 \log(9.467 \times 10^{-15}) \\
&= -140.24dB
\end{aligned}$$

Thus at $\Delta\omega = 1$ MHz from the carrier, the phase noise should be -140.24 dBc.

4.0 Oscillator Design Process

This section outlines the design process of the second voltage-controlled oscillator (VCO). For simplicity, the design can be broken down into the following components:

- Oscillator topology
- LC resonator
- Varactors
- Inductors
- Polyphase Frequency shifter

Each component is described in detail in the following sections. Throughout the design, emphasis was placed upon minimizing phase noise and power consumption and maximizing tuning range, as these tend to be the most important characteristics of a monolithic VCO [7].

4.1 The Negative G_m Oscillator

The first course of action was to select an appropriate topology to base the design of the oscillator upon. Though there are many common topologies available, such as the Hartley or the Colpitts oscillator, the negative transconductance (g_m) oscillator was selected because the design offers low phase noise and large amplitudes of oscillation [4]. The differential operation of this topology, in addition, also lowers the common mode power and the substrate noise [7].

As illustrated below in *Figure 4*, the negative g_m oscillator is comprised of an LC resonator and a pair of cross-coupled transistors. The LC resonator formed by the inductors and the capacitors set the oscillating frequency, while the cross-coupled

transistors create a negative resistance that sustains the oscillations. In addition, the current, represented in *Figure 4* by the ideal current source, sets the output voltage swing of the oscillations. This provides a starting point for design.

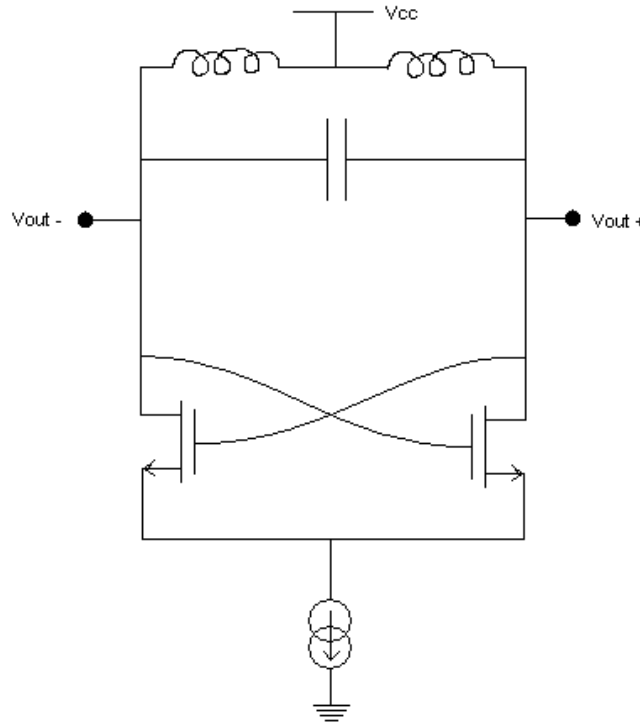


Figure 4: Negative G_m Oscillator topology

4.2 LC Resonator

Comprised simply of a capacitance in parallel with an inductance as illustrated below in *Figure 5*, the LC resonator produces the initial voltage oscillation in response to an impulse and controls the oscillating frequency. By representing the response to the impulse mathematically, the frequency of oscillation can be derived [1] to yield the following property:

$$\omega_{osc} = \frac{1}{\sqrt{LC}} \quad (4)$$

To enable the voltage-controlled oscillator to tune the oscillations to the desired frequency range, 1.82 GHz to 1.87 GHz in the case of the second VCO, the inductance and the capacitance of the resonator must be carefully set. To obtain an oscillating frequency of 1.82 GHz for the second VCO,

$$\begin{aligned} LC &= \left(\frac{1}{2\pi(1.82 \times 10^9)} \right)^2 \\ &= 7.647 \times 10^{-21} \end{aligned}$$

and, similarly, for 1.87 GHz, $LC = 7.244 \times 10^{-21}$.

To achieve these LC constants, the inductance of the resonator is set first. Since maximizing the inductances reduces the relative phase noise by increasing the voltage swing, it is desirable to make the inductance of the resonator as large as possible [5]. Larger inductances also inherently results in smaller capacitive values. This is desirable since smaller capacitances means lower power consumption [7]. This value, however, is limited by the self-resonant frequency of the inductor f_{res} , and by the fact that with large inductors, the required capacitance value will be almost achieved with the parasitic capacitances alone. This would leave no room for the capacitor used to tune the oscillating frequency [5]. As a result, the inductance of the resonator was set to 3nH.

Using a 3nH inductor, the required capacitance for an oscillating frequency of 1.82 GHz can now be calculated as follows from the LC constant:

$$\begin{aligned}
C &= \frac{7.647 \times 10^{-21}}{L} \\
&= \frac{7.647 \times 10^{-21}}{3 \times 10^{-9}} \\
&= 2.549 \text{ pF}
\end{aligned}$$

Similarly, a capacitance of 2.415 pF is required to set the frequency of oscillation to 1.87 GHz.

Figure 5 below illustrates the LC resonator:

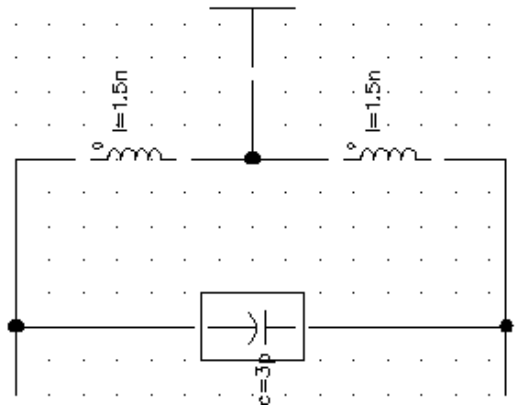


Figure 5: The LC Resonator

This design, however, is not yet complete, as the above LC resonator uses ideal inductors and fixed capacitors. In order to vary the frequency of oscillation, the fixed capacitor must be replaced by variable capacitors, known as varactors. As calculated above, these varactors must be able to vary between 2.415 pF and 2.549 pF. In addition, since real inductors vary with frequency, more realistic inductor models must be created to replace the ideal models of the simulator.

4.3 Varactors

Variable capacitors or varactors are used to tune the frequency of the oscillator. A MOS device, operating in accumulation mode and illustrated below in *Figure 6*, similar

to an NMOS transistor with its source and drain connected, accomplishes this by exploiting the natural capacitance between the gate and the substrate.

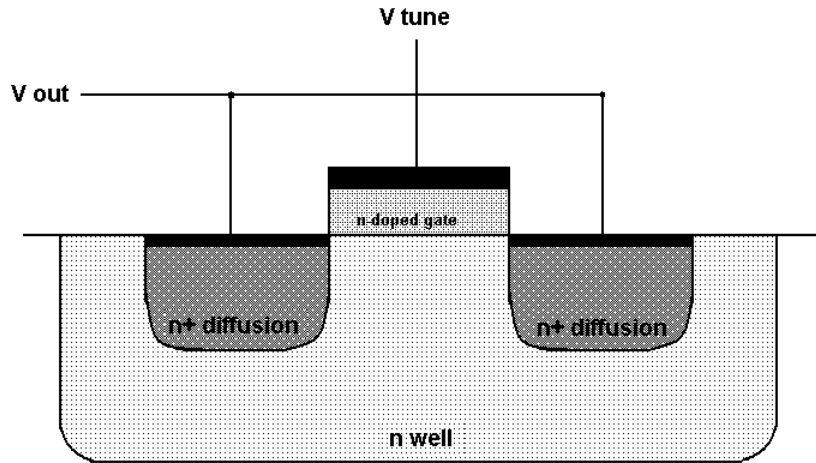


Figure 6: Cross-Section of a Varactor

With the “source” and “drain” terminals at the same potential, no current flows in the depletion region of the transistor. Thus, as the gate voltage is increased, the depletion region increases, in turn increasing the effective distance between the gate and the substrate. This, in turn, acts as a parallel plate capacitor. As illustrated by the following equation [3],

$$C = \frac{\epsilon_o \epsilon_r A}{d} \quad (5)$$

the capacitance of a parallel plate capacitor is inversely dependent upon the distance between the plates. Thus, as the gate voltage increases, the distance between the gate and the substrate increases causing a decrease in the capacitance.

In order to design the varactors to meet the tuning requirements of the second VCO, a test bench, illustrated in *Figure 7* below, was created to test the varactors.

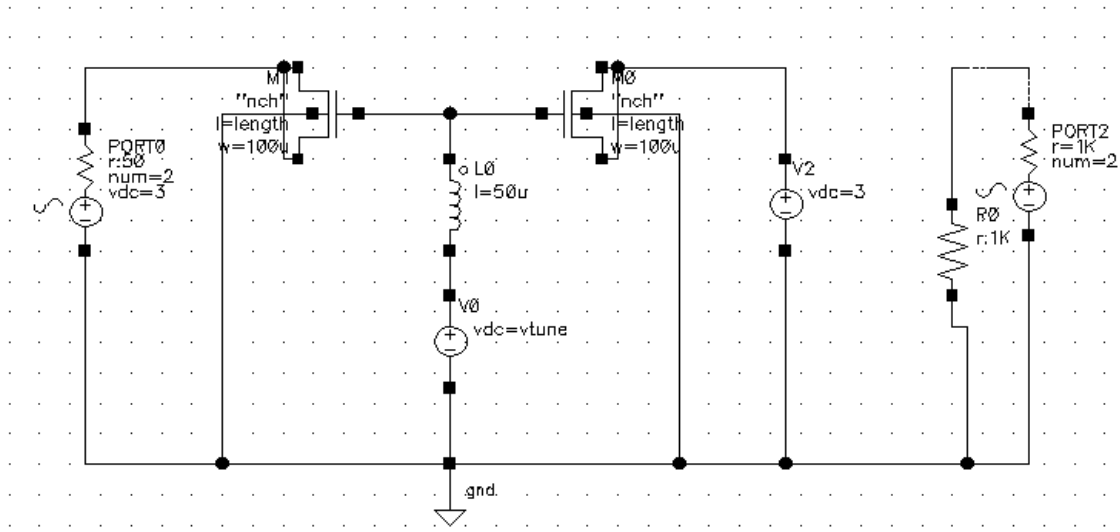


Figure 7: Varactor Test Bench

By running an s-parameter simulation on the above test bench and observing the S_{11} response, the input impedance (both real and imaginary components) could be determined as the tuning voltage V_{tune} was varied. The imaginary component of the input impedance is the capacitive characteristic of the circuit and is represented by the following relationship:

$$\text{Im}\{z\} = \frac{1}{\omega C_{\min}} \quad (6)$$

Based on varactors designed by Porret *et al.* [9] and Andreani *et al.* [10], the varactors for the VCO were dimensioned to have a width of $2630 \mu\text{m}$ and a length of $0.5 \mu\text{m}$. An s-parameter analysis was performed to obtain the following results:

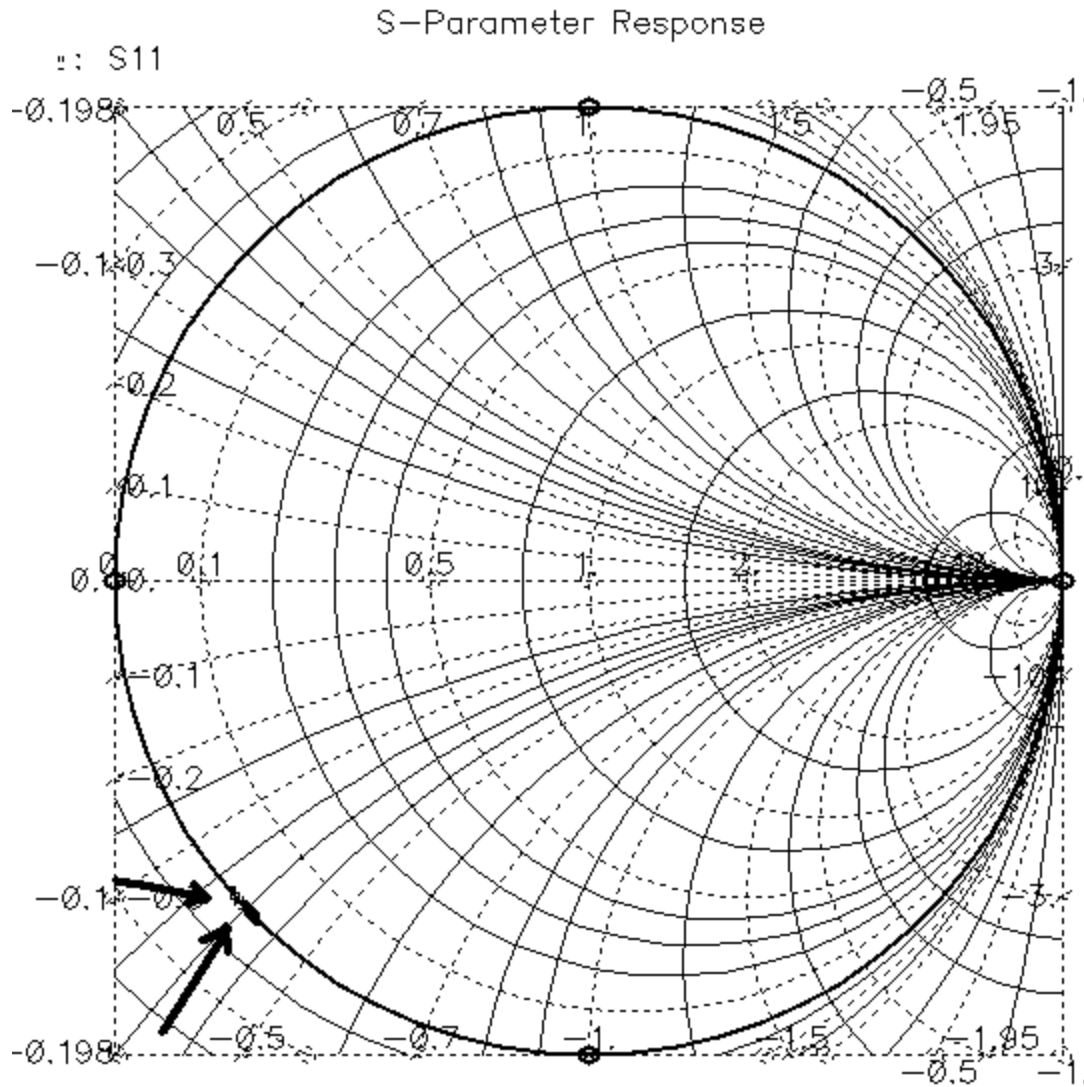


Figure 8: Smith Chart of Varactor's Input Impedance

From *Figure 8* above, the normalized impedance was found to be 0.7242 at 0V and 0.6889 at 3V. Since the test bench had $z_0 = 50 \Omega$, the capacitance of the varactors can be calculated. At 1.82 GHz, the capacitance C_{\min} is determined as follows:

$$\begin{aligned}
 \text{Im}\{z\} &= \text{Im}\{z_0 \tilde{z}\} \\
 &= (50\Omega)(0.7242) \\
 &= 36.210
 \end{aligned}$$

since,

$$\text{Im}\{z\} = \frac{1}{\omega C_{\min}}$$

$$C_{\min} = \frac{1}{2\pi(1.82\text{GHz})(36.210)}$$

$$= 2.415\text{pF}$$

In a similar fashion, C_{\max} can be determined to be 2.549 pF. Since the varactors can vary their capacitance between 2.415 pF and 2.549 pF for a given tuning voltage between 0 and 3 V, the specified swing in frequency of oscillation can be achieved.

To better illustrate this, the following figure, *Figure 9*, presents the capacitive variation with respect to the changing tuning voltage.

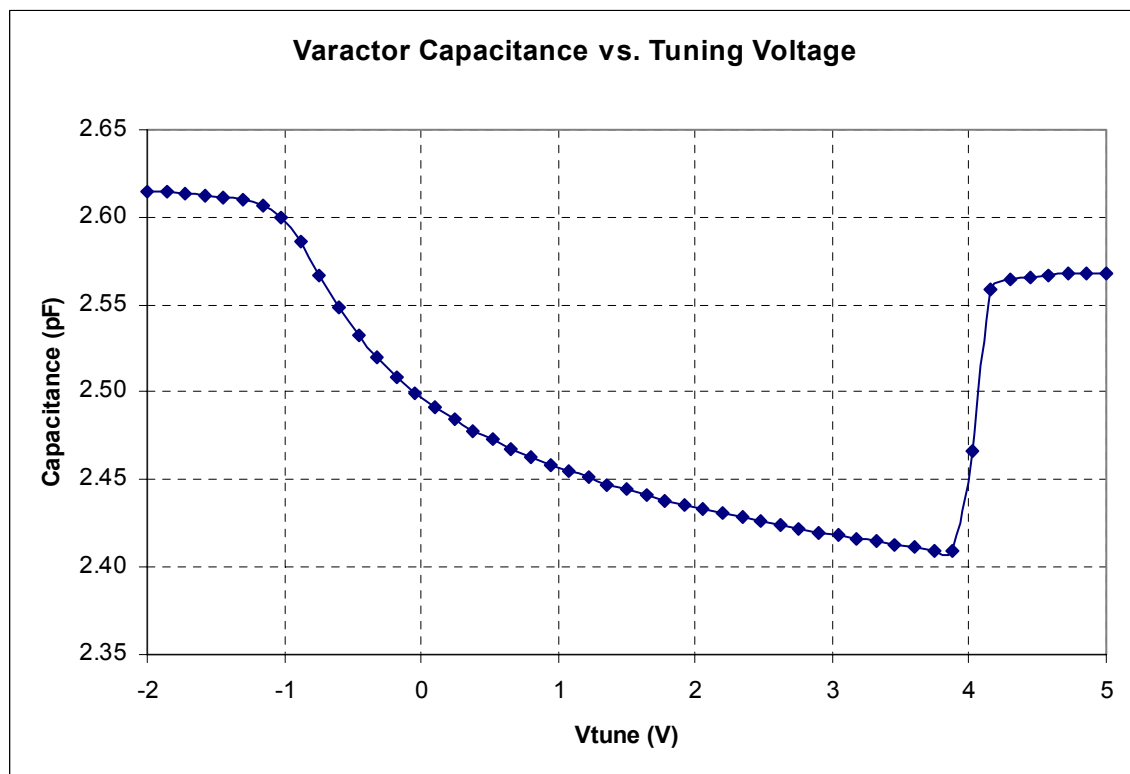


Figure 9: Normalized Imaginary Impedance vs. Tuning voltage of Varactors

4.4 Inductors

The phase noise in a voltage-controlled oscillator is primarily dependent upon the quality factor of the LC resonator [8]. Since a high quality factor (Q) is achievable for MOS varactors [9], the inductor is generally the source of the majority of the phase noise in the circuit. The quality factor of an inductor is defined by the following equation [1]:

$$Q_{ind} = \frac{|\text{Im}(Z_{ind})|}{|\text{Re}(Z_{ind})|} \quad (7)$$

$$= \frac{R_p}{\omega L} \quad (8)$$

As illustrated by the above equation, inductors with a high Q have very small parallel resistances associated with them and, consequently, less phase noise. Real inductors, however, tend to have much larger resistive properties and, thus, exhibit a significantly lower Q. On chip inductors, unfortunately, exhibit even lower values of Q; however, trends towards large-scale integration, lower costs, and lower power consumption have motivated much research and study [8].

From the definition of the quality factor Q above, it can also be observed that the Q of an inductor depends on the frequency of operation ω . This relationship however is not a linear one for all frequencies of operation. Care must be taken when designing an inductor to ensure that the frequency of operation does not exceed the self-resonance frequency f_{res} of the inductance, the point at which the coil can no longer be used as an inductor [8].

To ensure that the inductor achieves the desired inductance, self-resonance frequency, and sufficiently high Q, the following guidelines [8] were observed throughout the design of the inductor.

1. The width of the metal conductors was kept to a minimum
2. The center of the inductor was left hollow
3. The area occupied by the coil was kept to a minimum

Using the above guidelines, a variety of inductors were created and simulated using ASITIC. *Table 2* lists the geometry of the inductor that best met the specifications for the resonator.

Table 2: Inductor Geometry

Characteristic	Value
Radius	150 μm
Number of sides	20
Width of Trace	22 μm
Spacing	1 μm
Number of turns	4

The following figure is an illustration of the designed spiral inductor.

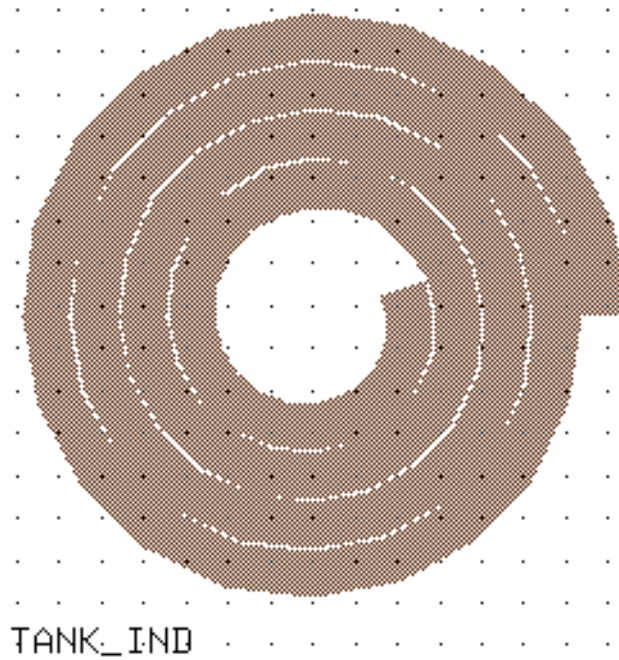


Figure 10: Inductor Geometry

Using a pi model simulation in ASITIC, the following operating points for this inductor were determined at 1.85 GHz, as indicated in the following table:

Table 3: Inductor Properties at 1.85 GHz

Characteristic	Value
Inductance, L	3.01 nH
Quality Factor, Q	5.22
Self-Resonance Frequency, f_{res}	4.52 GHz
Parallel Resistance, R_p	182.03 Ω

4.5 Polyphase Filters

As illustrated in *Figure 2*, the second voltage-controlled oscillator provides two reference tones to the image reject mixers. Each signal is at a frequency of 1.85 GHz, but one signal is 90 degrees out of phase from the other. This enables rejection of the image signal when the two signals are added together.

To implement this 90 degree phase shift, a polyphase filter is used because of its tolerance for component variations and improved performance over a wider range of frequencies [1]. The polyphase filter consists of a number of stages of RC networks, designed so that at a certain frequency all outputs are 90 degrees out of phase with each other. With each additional stage, the phase shifts become increasingly closer to 90 degrees. Typically, due to economic reasons, the number of stages is kept to a limit of four [11].

With the capacitors set to 100 pF, the resistor values were determined to be 1.162Ω from the following equation [1]:

$$\omega = \frac{1}{RC} \tag{9}$$

Figure 11 below illustrates the 3-stage polyphase filter implemented for this project.

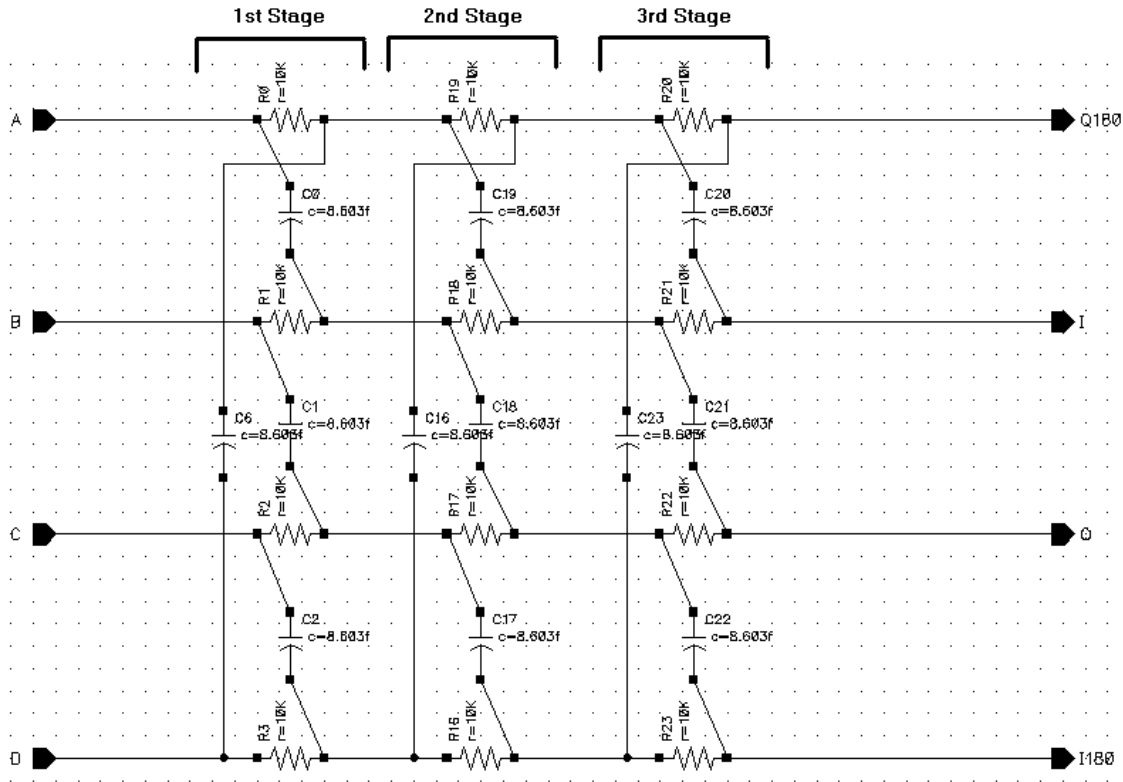


Figure 11: 3-Stage Polyphase Filter

To test the designed polyphase filter, the testbench illustrated below in *Figure 12*, was created and simulated. Below, a 1.85 GHz sinusoid is input into the polyphase filter. The signal into port C is 180 degrees behind port A.

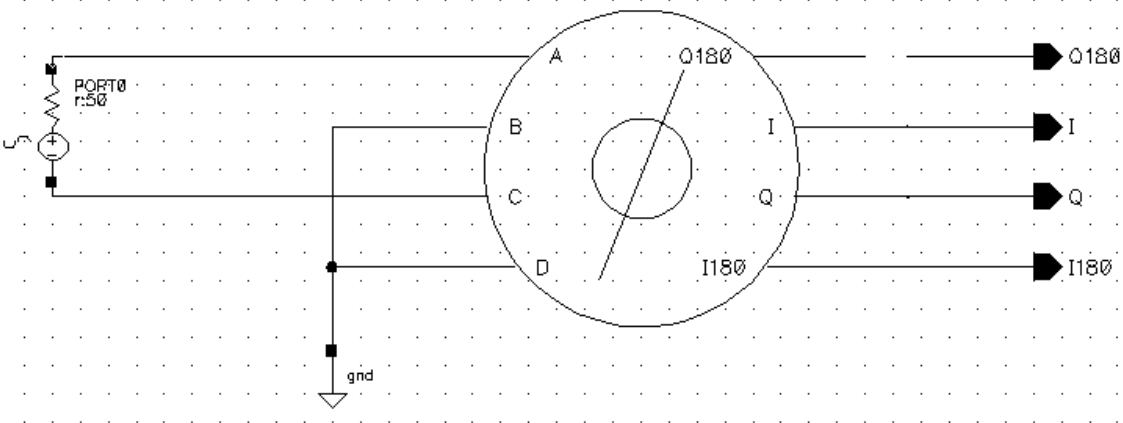


Figure 12: Polyphase Filter Testbench

The polyphase filter worked as expected as illustrated in *Figure 13* by the output signals obtained from port's I and Q. The time difference between the peaks of each output signal was measured to be 132.95 ps. Since a 1.85 GHz signal has a period of 540.54 ps, the phase shift can be calculated as follows,

$$\begin{aligned} \text{PhaseShift} &= \left(\frac{132.95 \text{ ps}}{540.54 \text{ ps}} \right) \times 360^\circ \\ &= (0.24595) \times 360^\circ \\ &= 88.545^\circ \end{aligned}$$

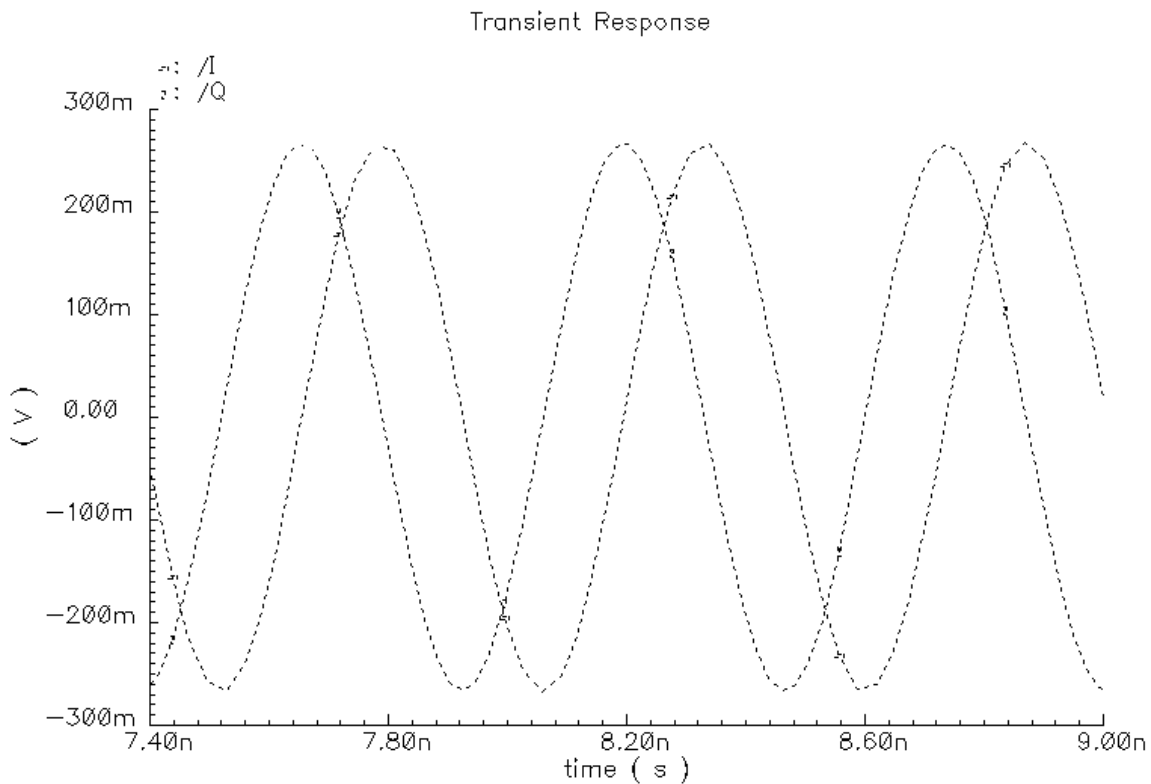


Figure 13: Polyphase Filter Testbench Output

5.0 Simulations and Results

This section presents the results of the simulations of the second oscillator. The figure below captures the operating points of all the transistors and components.

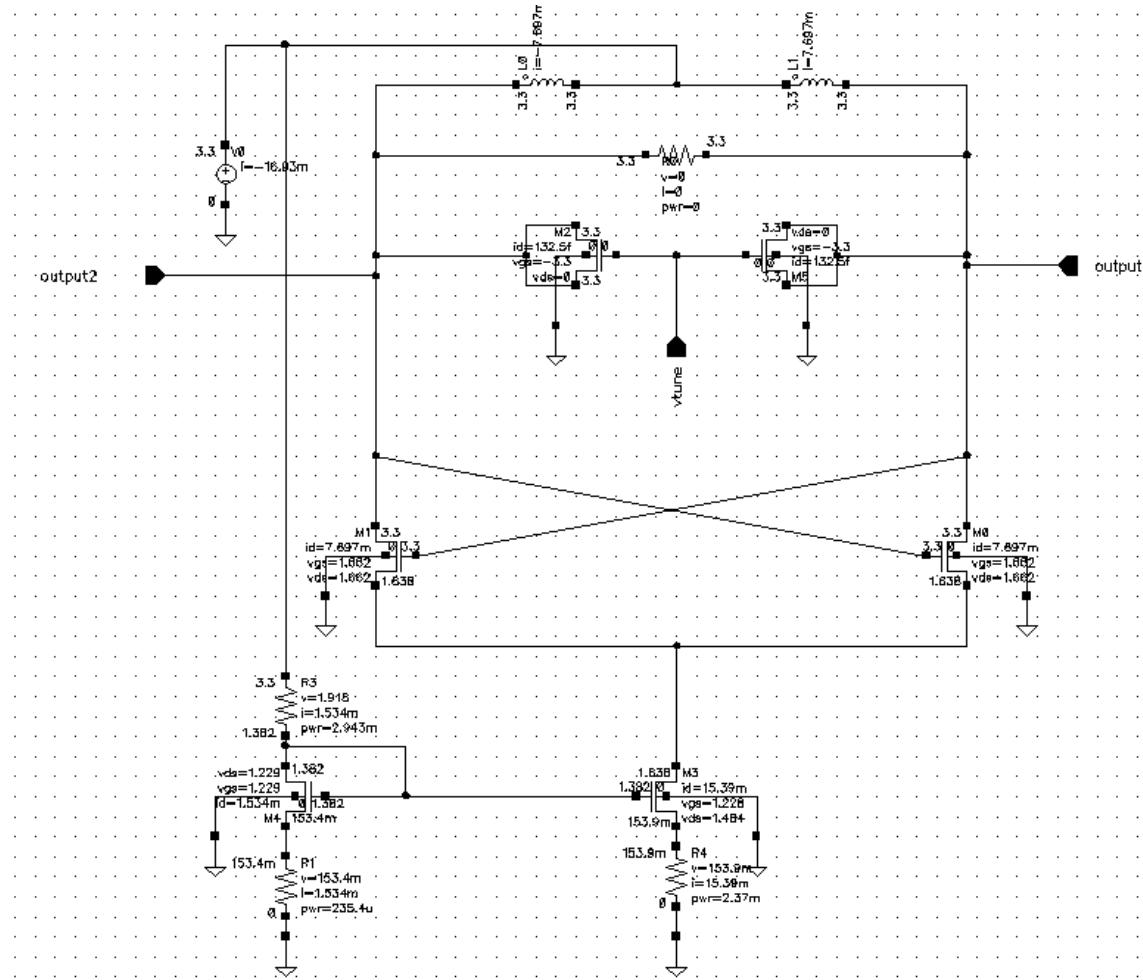


Figure 15: VCO Operating Points

5.1 Transient Response

The transient response of the cross-coupled negative g_m oscillator is illustrated below for $V_{\text{tune}} = 0$ V.

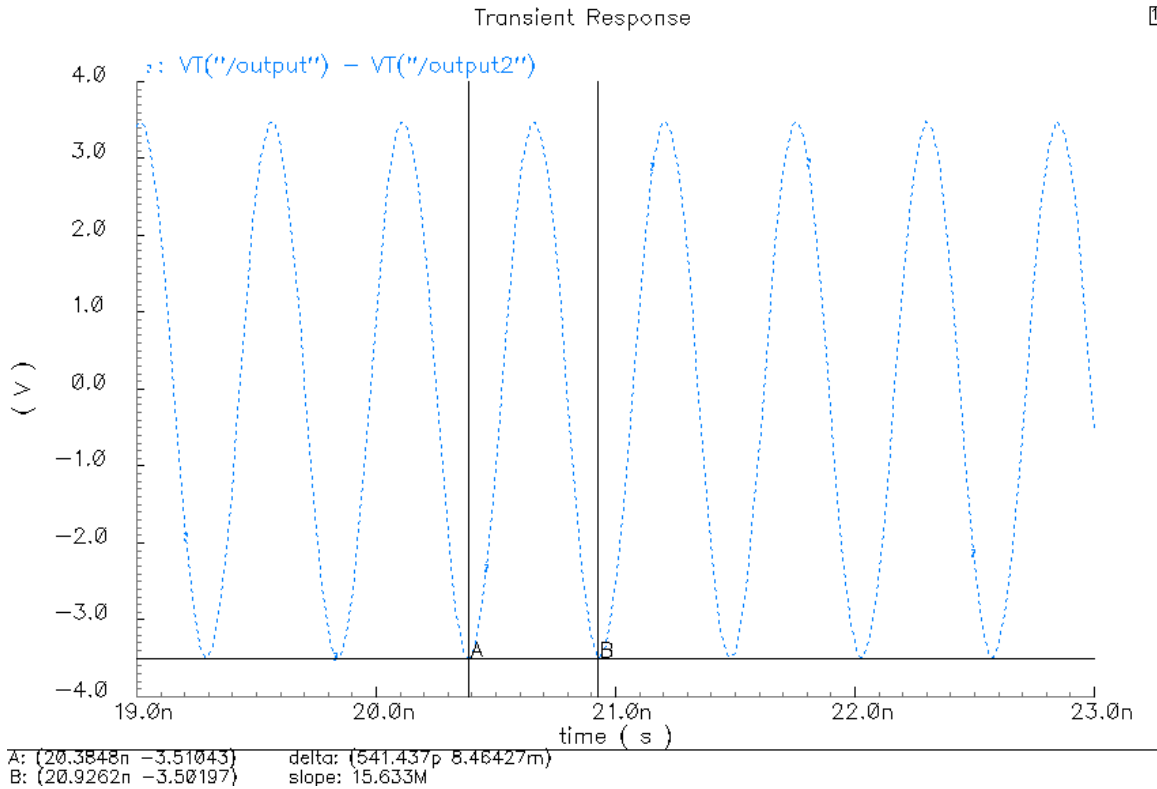


Figure 16: Transient Output Signal for $V_{\text{tune}} = 0$ V

From *Figure 16* above, the period was measured to be 541.437ps. Since frequency is the inverse of the period, the oscillating frequency can be calculated to be 1.847 GHz. Similarly, with the tuning voltage at 3 V, the oscillating frequency was measured to be 1.882 GHz. The output amplitude is also observed to be about 3.5 V.

5.2 Phase Noise

The phase noise simulation of the oscillator is presented below:

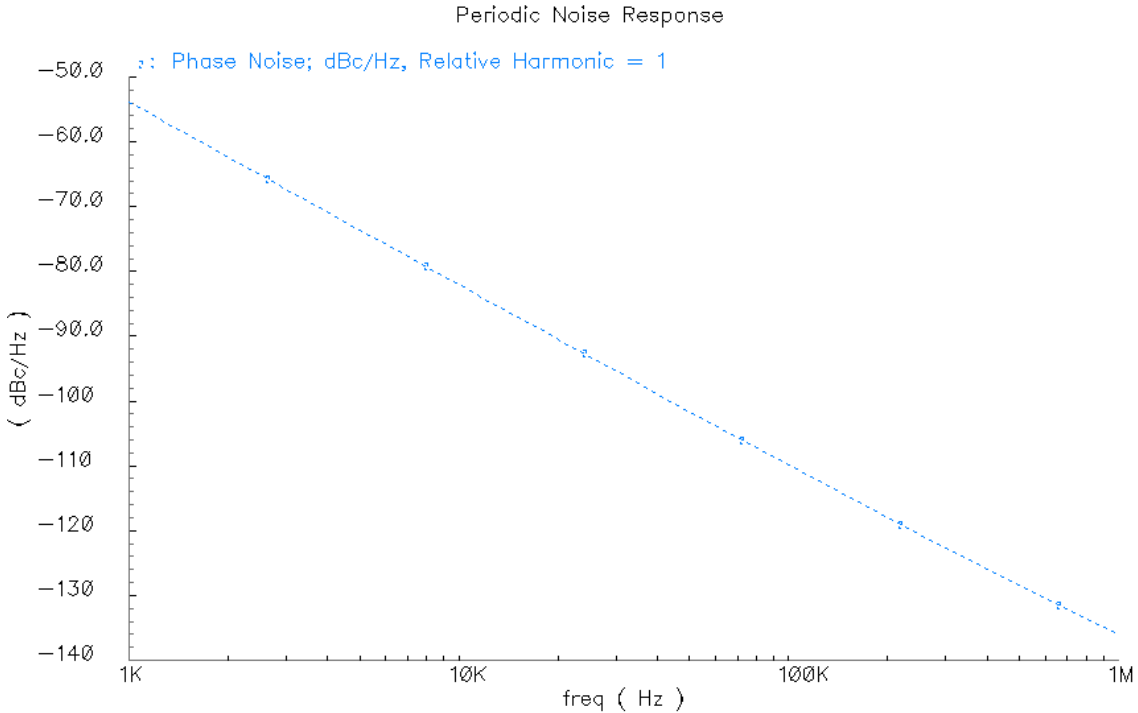


Figure 17: Phase Noise Response

The above figure illustrates the phase noise at certain frequencies away from the carrier. At 100 kHz away from the carrier, the phase noise is -109.9 dBc/Hz, and at 1 MHz, the phase noise drops to -136 dBc/Hz. These values indicate that there is slightly more noise in the circuit since the phase noise at 1 MHz offset was estimated using Leeson's equation to be -140.24 dBc.

5.3 Results Summary

The design results of the second voltage-controlled oscillator can be summarized in the following table:

Table 4: Summary of Results

Characteristic	Specification	Result
Oscillating Frequency	1.82 GHz to 1.87 GHz	1.847 GHz to 1.882 GHz
Current Drain	$I_{\text{Bias}} \leq 15 \text{ mA}$	15.39mA
Phase Noise	at 100 kHz, $\text{PN} \leq -103 \text{ dBc/Hz}$ at 1 MHz, $\text{PN} \leq -123 \text{ dBc/Hz}$	at 100 kHz, $\text{PN} = -109.9 \text{ dBc/Hz}$ at 1 MHz, $\text{PN} = -136 \text{ dBc/Hz}$

An entirely monolithic voltage-controlled oscillator was successfully designed in 0.18 μm CMOS to supply the image reject mixer with a stable, low-phase noise signal. The oscillating frequency can be tuned between 1.847 GHz and 1.882 GHz by varying a tuning voltage between 0V and 3V. Using a supply of 3.3 VDC, the circuit draws 15.39 mA of current and has phase noise of -109.9 dBc/Hz at a 100 kHz offset and -136 dBc/Hz at a 1MHz offset from the carrier. This is meets the requirements specified at the start of the project. To accomplish this, a spiral inductor was designed achieving a Q of 5.22. MOS varactors were also implemented.

Lastly, a three stage polyphase frequency shifter was designed to create a signal that was shifted by 90°. This design resulted in a phase shift of 88.545°.

6.0 Future Work

Unfortunately, due to computer difficulties beyond my control, I was unable to run a DRC simulation, thus making layout impossible. In addition to layout, other direction of future work could include modifying the existing design to meet the requirements of the first voltage-controlled oscillator, specifically, increasing the tuning range of the oscillator from 1.9 GHz to 2.7 GHz so that the VCO could be used to provide the reference tone for the upconverting mixer. In addition, it might be interesting to look at the design of the VCO using another technology such as BiCMOS or SiGe.

7.0 References

- [1] J. W. M. Rogers, C. Plett, *Radio Frequency Integrated Circuit Design*, Artech House Inc, Boston. In Press.
- [2] A. S. Sedra, K. C. Smith, *Microelectronic Circuits*, 1998, Oxford University Press, New York.
- [3] U. S. Inan, A. S. Inan, *Engineering Electromagnetics*, 1999, Addison-Wesley Inc, California.
- [4] J. W. M Rogers et al. "A Completely Integrated Cable Tuner". SiGe Semiconductors.
- [5] B. Razavi. "A 1.8 GHz CMOS Voltage Controlled Oscillator". *IEEE ISSCC Dig. Tech. Papers.* 23:6. Feb 1997. (p 388-389).
- [6] B. Razavi. "A Study of Phase Noise in CMOS Oscillators". *IEEE J. of Solid-State Circuits.* 31:3. March 1996. (p 331-343).
- [7] F. Svelto, S. Deantoni, and R. Castello. "A 1.3 GHz Low-Phase Noise Fully Tunable CMOS LC VCO". *IEEE J. on Solid-State Circuits.* 35:3. March 2000. (p 356-361).
- [8] J. Craninckx and S. J. Steyaert. "A 1.8 GHz Low-Phase-Noise CMOS VCO Using Optimized Hollow Spiral Inductors". *IEEE J. of Solid-State Circuits.* 32:5. May 1997. (p 736-744).
- [9] A. Porret et al. "Design of High-Q Varactors for Low-Power Wireless Applications Using a Standard CMOS Process". *IEEE J. of Solid-State Circuits.* 35:3. March 2000. (p 337-345)

- [10] P. Andreani and S. Mattison. “On the Use of MOS Varactors in RF VCO’s”.
IEEE J. of Solid-State Circuits. 35:6. June 2000. (p 905-910).
- [11] M. J. Gingell. “Single Sideband Modulation using Sequence Asymmetric
Polyphase Networks”. *Electrical Communications*. 48. 1973. (p 21-25).